FULL PAPER

BJC

British Journal of Cancer (2018) 118, 43–51 | doi: 10.1038/bjc.2017.374

Keywords: acetyl-CoA carboxylase; cancer; metabolism; membrane characteristics; metastasis; soraphen A; proliferation; tumour growth

Targeting *de novo* lipogenesis as a novel approach in anti-cancer therapy

Katharina Stoiber[1,2], Olga Nagło[1], Carla Pernpeintner[2,3], Siwei Zhang[1], Andreas Koeberle[4], Melanie Ulrich[1], Oliver Werz[4], Rolf Müller[5], Stefan Zahler[1], Theobald Lohmüller[2,3], Jochen Feldmann[2,3] and Simone Braig*[,1]

[1]*Department of Pharmacy, Pharmaceutical Biology, Ludwig-Maximilians-University of Munich, Butenandstr. 5-13, Munich, Germany;* [2]*Nanosystems Initiative Munich (NIM), Schellingstraße 4, Munich, Germany;* [3]*Photonics and Optoelectronics Group, Department of Physics and Center for Nanoscience, Ludwig-Maximilians-University of Munich, Amalienstr. 54, Munich, Germany;* [4]*Chair of Pharmaceutical/Medicinal Chemistry, Institute of Pharmacy, Friedrich-Schiller-University Jena, Philosophenweg 14, Jena, Germany and* [5]*Department of Microbial Natural Products, Helmholtz Institute for Pharmaceutical Research Saarland, Helmholtz Centre for Infection Research and Department of Pharmaceutical Biotechnology, Saarland University, Campus E8.1, Saarbrücken, Germany*

Background: Although altered membrane physiology has been discussed within the context of cancer, targeting membrane characteristics by drugs being an attractive therapeutic strategy has received little attention so far.

Methods: Various acetyl-CoA carboxylase 1 (ACC1), and fatty acid synthase (FASN) inhibitors (like Soraphen A and Cerulenin) as well as genetic knockdown approaches were employed to study the effects of disturbed phospholipid composition on membrane properties and its functional impact on cancer progression. By using state-of-the-art methodologies such as LC-MS/MS, optical tweezers measurements of giant plasma membrane vesicles and fluorescence recovery after photobleaching analysis, membrane characteristics were examined. Confocal laser scanning microscopy, proximity ligation assays, immunoblotting as well as migration, invasion and proliferation experiments unravelled the functional relevance of membrane properties *in vitro* and *in vivo*.

Results: By disturbing the deformability and lateral fluidity of cellular membranes, the dimerisation, localisation and recycling of cancer-relevant transmembrane receptors is compromised. Consequently, impaired activation of growth factor receptor signalling cascades results in abrogated tumour growth and metastasis in different *in vitro* and *in vivo* models.

Conclusions: This study highlights the field of membrane properties as a promising druggable cellular target representing an innovative strategy for development of anti-cancer agents.

Cellular membranes are not only selective barriers that mediate structural cell integrity and compartmentalisation, but are also signalling platforms for membrane bound and integral membrane proteins controlling pivotal processes including cell growth, differentiation and migration (Cooper, 2000). Recent reports suggesting that cellular membranes are involved in regulation of malignancy and metastatic competence of tumour cells have set the stage to exploit the membrane as a therapeutic target (Escriba *et al*, 2015). Deformability of cancer cells, which is determined by membrane characteristics as well as the cytoskeleton, was proposed as a novel marker to grade metastatic potential (Remmerbach *et al*, 2009; Swaminathan *et al*, 2011).

The main efforts to change cell deformability have so far largely concentrated on targeting cytoskeletal components (Suresh, 2007). Though, membrane characteristics also impact cell biomechanics and are strongly regulated by the cellular lipid composition. In line with the study performed by Rysman and colleagues, we were able to demonstrate that inhibiting acetyl-CoA carboxylase (ACC), the

*Correspondence: Dr S Braig; E-mail: simone.braig@cup.uni-muenchen.de

Received 5 July 2017; revised 22 September 2017; accepted 22 September 2017; published online 7 November 2017

rate limiting enzyme of fatty acid synthesis, influences the phospholipid composition of cellular membranes, and thus affects membrane properties (Rysman *et al*, 2010; Braig *et al*, 2015).

The aim of this study was to unravel the direct consequences of disturbed membrane physiology on membrane-associated key players of cancer-promoting signalling pathways and its functional impact on tumour growth and metastasis *in vitro* and *in vivo*. Thereby, we were able to shed light on the molecular basis of targeting membrane properties as a promising therapeutic strategy in the development of new molecular approaches against cancer.

MATERIALS AND METHODS

Drugs and antibodies. Soraphen A was provided by the authors (Prof Dr Rolf Müller, Saarbrücken, Germany). TOFA, Cerulenin, CP-640,186, C75 and UCM05 were purchased from Sigma-Aldrich (St Louis, MO, USA). For nuclei staining Hoechst33342 (Sigma-Aldrich) was used. Antibodies against ACC1, HER2, pHER2 and pEGFR were obtained from Cell Signaling Technology (Danvers, MA, USA). The EGFR and the actin antibody were purchased from Merck Millipore (Billerica, MA, USA). For immunostaining and immunoblotting following secondary antibodies were used: Alexa Fluor 488-conjugated mAb18, Alexa Fluor 546-conjugated mAb18 and Alexa Fluor 633-conjugated mAb18 (Thermo Fisher Scientific Inc., Waltham, MA, USA), HRP-goat-anti-Mouse (Santa Cruz Biotechnology, Santa Cruz, CA, USA) and HRP-goat-anti-Rabbit (Bio-Rad, Hercules, CA, USA).

Cell culture. The mammary carcinoma cell lines SKBR3 and MDA-MB-231 were obtained from Cell Line Services (CLS, Eppelheim, Germany). The hepatocellular carcinoma cell line Huh7 was purchased from the Japanese Collection of Research Bioresources (JCRB, Osaka, Japan) and T24 bladder carcinoma cells were obtained from the German Collection of Microorganisms and Cell Cultures (DSMZ, Braunschweig, Germany), respectively. The mammary epithelial cell line MCF10a was obtained from ATCC (Manassas, VA, USA). All cell lines were cultured in DMEM media supplemented with 10 % foetal calf serum and 1 % penicillin/streptomycin (P/S).

Analysis of phospholipids by liquid chromatography ESI tandem mass spectrometry. Extraction and analysis of phospholipids were performed as described previously (Koeberle *et al*, 2013). In brief, extracted phospholipids were separated on an Acquity UPLC BEH C8 column (1.7 μm, 1 × 100 mm, Milford, MA, USA) using an Acquity Ultraperformance LC system (Waters), which was coupled to a QTRAP 5500 Mass Spectrometer (Sciex, Framingham, MA, USA) equipped with an electrospray ionisation source. The two fatty acid anion fragments of phospholipids were detected by multiple reaction monitoring in the negative ion mode; the most intensive transition was used for quantification. Our method was optimised to compare phospholipid profiles and not for absolute quantification. Mass spectra were processed using Analyst 1.6 (Sciex).

Giant plasma membrane vesicle deformation. Cells were grown in 40 mm dishes and treated with 5 μM soraphen A for 72 h. Culture medium was discarded and cells were washed twice with PBS. To induce vesiculation 600 μl of buffer solution containing 150 mM NaCl (Sigma-Aldrich, S7653), 10 mM 2-(4-(2-hydroxyethyl)-1-piperazinyl)-ethanesulfonic acid (Sigma-Aldrich), 2 mM $CaCl_2$ (Sigma-Aldrich), 8 mM di-thiothreitol (Roth, Karlsruhe, Germany) and 1 M paraformaldehyde (Sigma-Aldrich) was added and the cells were incubated in a shaker (37 °C, 5% CO_2 and 60 cycle min^{-1}) for 2 h. After shaking, the upper 3/4 of the solution was removed and used for analysis.

Membrane deformability was measured by analysing vesicle deformation in elongational counter flow for vesicles with a diameter between 3.5 and 10 μm. For a more detailed description of the laser microscopical method, please also see Pernpeintner *et al* (2017). A 1064 nm laser (Cobolt AB, Cobolt Rumba, 05-01 series) was coupled through a water immersion objective of an upright dark-field microscope (ZEISS, Axiovert, Oberkochen, Germany) to optically trap individual cell-membrane vesicles. Video imaging was done with a Canon 6D digital camera. Moving the motorised stage (Linos, Göttingen, Germany) with velocities up to a few 10 μm s^{-1} led to a constant counter flow in the sample and in consequence, deformation of the trapped vesicle that could be fitted with an ellipse in the 2D projection. For each measured vesicle, the flow speed was increased until the deformation of the vesicle saturated at a maximum deformation value D_{max} with a and b being the half-axis of an ellipse:

$$D_{max} = \frac{|a-b|}{a+b}$$

Confocal laser scanning microscopy. SKBR3 cells were treated as indicated, fixed with methanol for 10 min at −20 °C and washed three times with PBS. After blocking the unspecific binding sites with 2% BSA, primary antibodies were incubated for 2 h at room temperature. Rhodamine phalloidin was used to stain F-actin. Cells were washed three times with PBS, incubated with secondary antibodies for 1 h and mounted with FluorSave Reagent mounting medium (Merck, Darmstadt, Germany). Nuclei were stained with Hoechst33342.

Fluorescence recovery after photobleaching analysis. To assess lateral membrane fluidity, fluorescence recovery after photobleaching (FRAP) analysis was performed. Therefore, cells were transfected with the plasmid pMyrPalm-mEGFP by electroporation (gift from Daniel Gerlich (Steigemann *et al*, 2009) obtained from Addgene, Cambridge, MA, USA, #21038) in order to visualise cellular membranes. Transfected cells were stimulated with soraphen A or siACC1 for 72 h and cultivated in starvation medium 24 h before imaging. The cells were placed into a humidified climate chamber of a TCS SP8 ZSMD microscope (Leica, Wetzlar, Germany) and incubated during microscopy at 37 °C and 5% CO_2. Regions of interest were defined in treated and untreated cells and bleached by maximum laser energy at 488 nm. After photobleaching the fluorescence recovery was monitored for 10 min, taking an image every 10 s.

Evaluation of receptor dimerisation. To analyse receptor dimerisation and dimer localisation, Duolink proximity ligation assay (Sigma-Aldrich) was used according to the manufacturer's instructions. Briefly, cells were stimulated for 72 h with soraphen A and starved 24 h before analysing. To evaluate EGFR-HER2 dimerisation, cells were fixed with methanol for 10 min at −20 °C, washed three times and blocked with 2% BSA for 10 min at RT. Primary antibodies were diluted 1 : 100 in blocking solution and added to the cells. After three washing steps the samples were incubated with PLA probes for 1 h at 37 °C. Ligation was performed at 37 °C for 30 min and the amplification reaction was conducted at 37 °C for 100 min. Before fixation the nuclei were stained with Hoechst33342 (Sigma-Aldrich). Receptor dimerisation was analysed by confocal microscopy.

Receptor recycling assay. Cells were stimulated with soraphen A or transfected with siACC1 for 72 h. Subsequently, rhodamine-conjugated Transferrin (Invitrogen, Thermo Fisher, Waltham, MA, USA) diluted 1 : 100 in PBS and Hoechst33342 was added to the cells and incubated for 1 h in 37 °C. Cells were washed three times with PBS. Acidic wash solution (0.5 M NaCl and 0.2 M of acetic acid) was added for 5 min (shaking) to remove excess of rhodamine-Transferrin not absorbed by cells. After further

washing steps, cells were fixed with 4% PFA, mounted with FluorSave Reagent (Merck) and analysed by confocal laser scanning microscopy.

Heterogeneity of EGFR. MDA-MB-231 cells were treated with soraphen A for 4 h, detached and reseeded in chemotaxis μ-slide. A chemotactic gradient between 0 and 10% FCS was established. Migrating cells were fixed after 16 h with 4% PFA and stained with EGFR antibody, rhodamine phalloidin and Hoechst33342. Cells were imaged and heterogeneity of EGFR localisation was analysed by using ImageJ software tool. Thereby, heterogeneity is described as the fraction of pixels in the cell that deviate more than 10% from the average intensity.

Immunoblotting. Cells were harvested in lysis buffer supplemented with the protease inhibitor cocktail Complete (Sigma-Aldrich), 1 mM PMSF and 2 mM Na_3VO_4. Proteins (30 μg) were separated by SDS–PAGE and blotted to nitrocellulose membranes. Nonspecific binding sites were blocked with 5% milk powder in TBS. Blots were incubated with primary antibodies for 2 h at RT. Incubation with secondary horseradish peroxidase-conjugated antibodies followed after washing steps for 2 h at room temperature. Proteins were visualised by the chemiluminescence-based ECL detection system (GE Healthcare, Buckinghamshire, UK) or the ChemiDoc Touch Imaging system (Bio-Rad). As a loading control actin or unstained gel was used. Western blots were quantified with ImageJ or the Image Lab Software (Bio-Rad).

Rescue experiments. Cells were seeded in 24-well plates and treated with 10 μM of soraphen A for 24 h in DMEM with 2% of FCS. The PI mix was prepared from L-α-phosphatidylinositol ammonium salt from bovine liver dissolved in chloroform (Sigma-Aldrich). After removal of chloroform under a nitrogen stream, HEPES buffer (20 μM) was added, and the mixture was kept for 30 min in a water bath (37 °C) to hydrate PIs. Growth medium was added and the incubation continued for 30 min in a water bath at 37 °C. Afterwards, the PI mix was sonicated (30 min) and immediately added to the cells. After 16 h, the PI-containing medium was replaced by fresh medium with 2% FCS and 1% P/S. The proliferation of cells was analysed using CellTiter-Blue reagent (Promega) after additional 48 h.

Further *in vitro* assays. Please refer to Supplementary Material.

***In vivo* dissemination assay.** 4T1-luc cells were pretreated with 25 nM soraphen A for 72 h, detached and resolved in PBS. 1×10^5 cells were injected i.v. into the tail vein of eight 6-week old Balb/c mice (Harlan Laboratories GmbH, Eystrup, Germany). Four days after injection, mice were anesthetised and bioluminescence of luciferase tagged cells was measured 10 min after luciferin injection by using the IVIS Spectrum system (Caliper Life Science, Hopkinton, MA, USA). Total flux/area was determined as photons second cm^{-2}.

***In vivo* xenograft mouse model.** Hepatocellular carcinoma cells Huh7 were harvested, 3×10^6 cells were dissolved in 100 μl PBS and injected into the flank of 20 eight-week-old SCID mice (Charles River Laboratories, Wilmington, MA, USA). After tumours have developed, 10 mice were treated i.p. daily with 40 mg kg^{-1} soraphen A dissolved in 5% DMSO, 10% solutol and PBS for 9 days. Tumour volume was assessed by using a digital caliper; thereby length (l), wide (w) and height (h) of the tumour was measured. The tumour volume was calculated by the formula $V = (\pi/6) \cdot l \cdot w \cdot h$.

RESULTS

Modulation of phospholipid composition affects membrane properties. In order to confirm and extend previous studies investigating the influence of abrogating fatty acid biosynthesis by using the ACC1 inhibitor soraphen A on membrane characteristics of cancer cells (Rysman *et al*, 2010; Braig *et al*, 2015), ultra-performance liquid chromatography-coupled ESI tandem mass spectrometry of phospholipids isolated from SKBR3 breast cancer cell lines was conducted. As demonstrated in Figure 1A, treatment with soraphen A significantly reduces total amounts of phosphatidylcholine (PC), -ethanolamine (PE) and -inositol (PI) species and results in a shift towards polyunsaturated and long chain fatty acids (Figure 1B and C, detailed analysis is shown in Supplementary Figure S1). By optical trapping of giant plasma membrane vesicles by a laser beam and application of an elongational counter flow at a distinct flow speed, the maximal deformation of membranes was analysed (Figure 1D, Supplementary Figure S2A). Giant plasma membrane vesicles generated from soraphen A-treated SKBR3 cells show an impaired deformation compared to control cells (Figure 1E, representative images of the vesicles are shown in Supplementary Figure S2B). Next, SKBR3 cells were transfected with a pMyrPalm-mEGFP vector and the lateral fluidity of the plasma membrane was assessed by FRAP analysis. Impeding ACC1 activity by soraphen A or RNA interference results in a decreased membrane fluidity (Figure 1F), hence indicating that altering phospholipid profiles impairs membrane mechanics.

Impairment of receptor dimerisation and recycling. In the following set of experiments, the consequences of altered membrane composition on main tasks of cellular membranes were elucidated. In order to investigate the dimerisation of the growth factor receptors HER2 and EGFR upon treatment of SKBR3 cells with soraphen A, we employed the Duolink Proximity Ligation assay, which enables HER2-EGFR dimer visualisation *in situ*. Thereby, soraphen A treated and untreated cells were incubated with specific EGFR and HER2 antibodies. PLA probes, tagged to the respective secondary antibodies, in addition with DNA oligonucleotides and ligation enzymes enable rolling circle amplification leading to fluorescent dots when the two proteins are in close proximity. As expected, stimulation of the cells with 100 ng ml^{-1} EGF for 15 min revealed a strong induction of EGFR–HER2 interaction (Figure 2A). As shown in Figure 2B and C, the signal intensity of HER2-EGFR complexes and the number of HER2-EGFR clusters per cell is significantly reduced in soraphen A-treated cells, whereas the size of the clusters is unaffected after inhibiting ACC1 (Figure 2D). Interestingly, beyond impairing dimerisation of transmembrane receptors, we observed that inhibition of ACC1 weakens recycling processes. Treatment with of SKBR3 cells with soraphen A (Figure 2E) and knockdown of ACC1 (Figure 2F, successful downregulation of ACC1 is shown in Supplementary Figure S3) results in an accumulation of the receptor ligands in the perinuclear compartment as investigated by using rhodamine coupled transferrin-complexes as a model system. As a result of diminished receptor dimerisation and recycling processes, activation of tumour relevant growth factor signalling cascades like EGFR and HER2 is clearly reduced upon treatment of SKBR3 breast cancer cells with the ACC1 inhibitor soraphen A (Figure 2G). As aberrant EGFR and HER2 activation influence downstream signalling cascades being decisive in tumour biology, we analysed two main functional aspects in cancer progression, namely migration and proliferation processes.

Inhibition of cancer cell migration and invasion. Highly metastatic MDA-MB-231 breast cancer cells were transfected with siRNA against ACC1 and migratory and invasive potential was assessed. As shown in Figure 3A, inhibiting the mRNA expression of ACC1 strongly impairs the migration and invasion of MDA-MB-231 cells as assessed in Boyden chamber assays. Consistently,

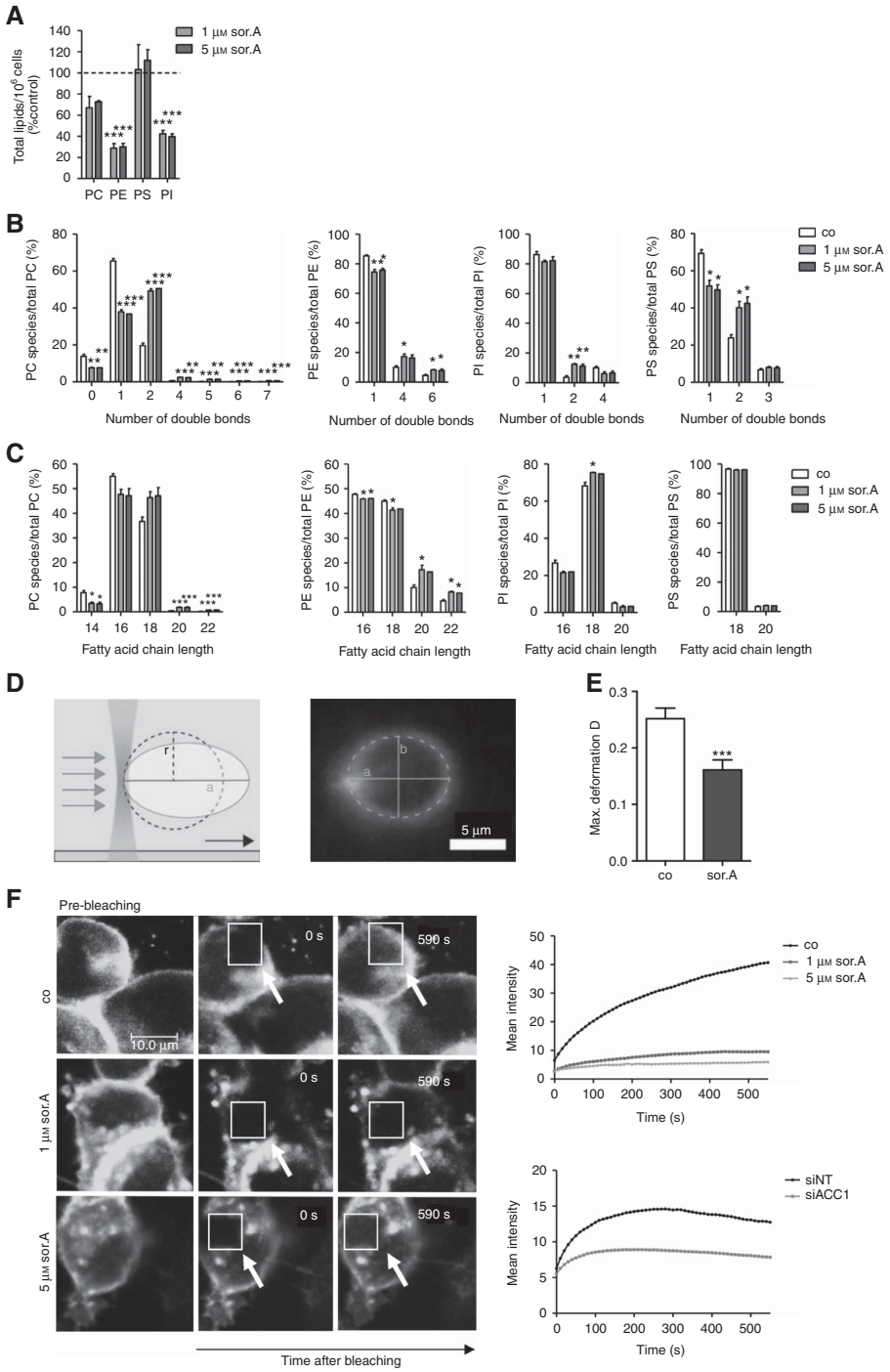

Figure 1. Cell mechanics is strongly influenced by ACC1 inhibition. (**A**) Lipids of soraphen A-treated SKBR3 cells (72 h) were extracted and analysed by liquid chromatography ESI tandem mass spectrometry. Total signal intensities of phospholipid subclasses in soraphen A-treated cells were normalised to control. A value of 100% was assigned to the signal intensities of control cells. (**B**) Effect of soraphen A on the number of double bonds in fatty acids and (**C**) the fatty acid chain length of the major phospholipid subclasses phosphatidylcholine (PC), phosphatidylserine (PS), phosphatidylethanolamine (PE) and phosphatidylinositol (PI). Signal intensities are shown relative to the total phospholipid subclass intensity. (**D**) Experimental setup for vesicle deformation measurements: A single membrane vesicle derived from SKBR3 cells is trapped on one end with a focused laser beam (optical tweezer). Application of flow results in elongation of the vesicle along the flow direction. Right: Dark-field microscopy image of an optically trapped vesicle. The 2D projection of the vesicle is fitted with an ellipse using home-built Matlab and C++ routines. A dashed line indicates an elliptic fit of the vesicle cross-section with half axis *a* and *b*. (**E**) Comparison of the maximum deformation D_{max} of vesicles obtained from cells after treatment with soraphen A or control. The error bars indicate the s.e.m. for a sample size of 30 and 40 cells, respectively. (**F**) Lateral membrane fluidity was assessed by FRAP assay in soraphen A-treated SKBR3 cells and after siACC1 transfection, respectively. Representative images are depicted on the left. White arrows indicate the photobleached area. Right: mean fluorescence recovery after photobleaching is diagrammed over time. Statistical analysis was performed using Student's *t* test: $*P<0.05$, $**P<0.01$, $***P<0.001$.

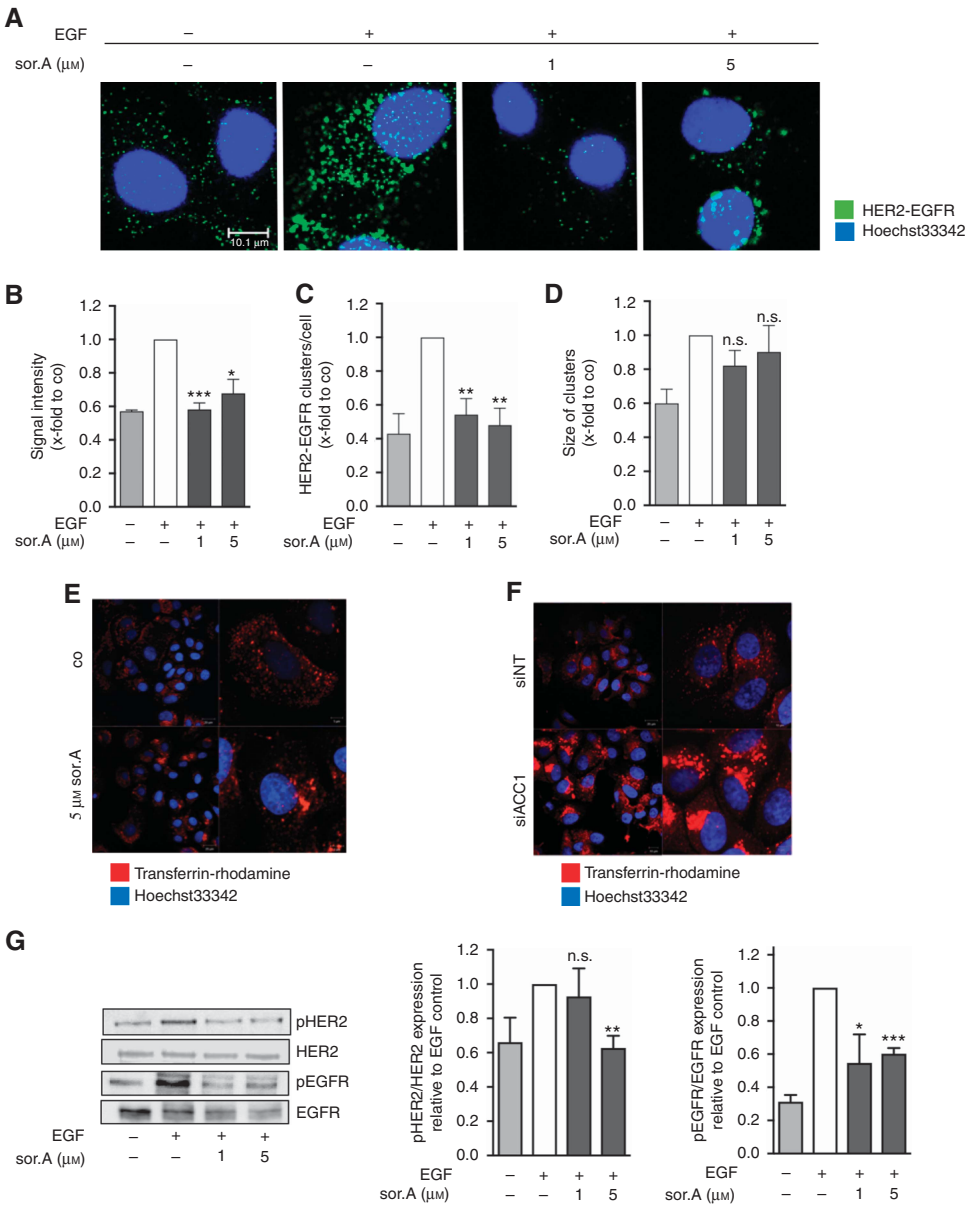

Figure 2. Impaired dimerisation, recycling and activation of transmembrane receptors. (**A**) HER2-EGFR dimerisation of SKBR3 cells treated for 72 h with soraphen A was determined by proximity ligation assay. (**B**) Signal intensity, (**C**) the number of EGFR-HER2 clusters and (**D**) cluster size were analysed by ImageJ. (**E**) Receptor recycling of soraphen A-treated and (**F**) siACC1-transfected SKBR3 cells was monitored by adding rhodamine-tagged transferrin. (**G**) SKBR3 cells were stimulated with soraphen A for 72 h and phosphorylation of HER2 and EGFR was evaluated by western blot analysis. Prior to lysis cells were stimulated with 100 ng ml^{-1} EGF for 15 min. Statistical analysis was performed using Student's *t* test: n.s. = non-significant, *$P<0.05$, **$P<0.01$, ***$P<0.001$.

treatment of the cells with the chemical ACC inhibitor TOFA and the FASN blocker Cerulenin results in significant abrogation of cell migration (Figure 3B). Interestingly, migratory potential of the mammary epithelial cell line MCF10a is not affected by soraphen A (Figure 3C). Detailed analysis of the migratory behaviour of soraphen A-treated cells revealed that whereas the overall velocity of the cells is not affected, the directed migration (displayed as forward migration index) towards FCS and EGF as chemoattractant is strongly reduced upon treatment of MDA-MB-231 and T24 cells with ACC inhibitor (Figure 3D, Supplementary Figure S4a). These results could be obtained not only in 2D chemotaxis assays, but also after embedding the cells into Matrigel (Figure 3E, Supplementary Figure S4b). In addition, we analysed the effect of soraphen A on the invasive capacity of three-dimensional spheroids into a collagen matrix. Therefore, T24 bladder carcinoma cells were grown as spheroids, stimulated with soraphen A, and embedded in collagen. After 3 days, diminished invasion of the soraphen A-treated cells into the surrounding matrix following FCS as chemoattractant was observed (Figure 3F). Detailed evaluation of the chemotactic migration of MDA-MB-231 cells towards EGF revealed that the heterogenous expression of the EGF-receptor (analysed by staining with a specific EGFR antibody and quantified as described in the Materials and Methods section), which is known to be primarily located at the leading edge of migrating cells, is compromised upon treatment with soraphen A (Figure 3G). This finally results in abrogation of EGFR phosphorylation (Supplementary Figure S5). Furthermore, treatment with the ACC inhibitor impairs the formation of filopodia, actin-containing cytoplasmic projections being important for migration and attachment, as shown by staining of spreading MDA-MB-231 breast cancer cells with rhodamine-phalloidin (Figure 3H).

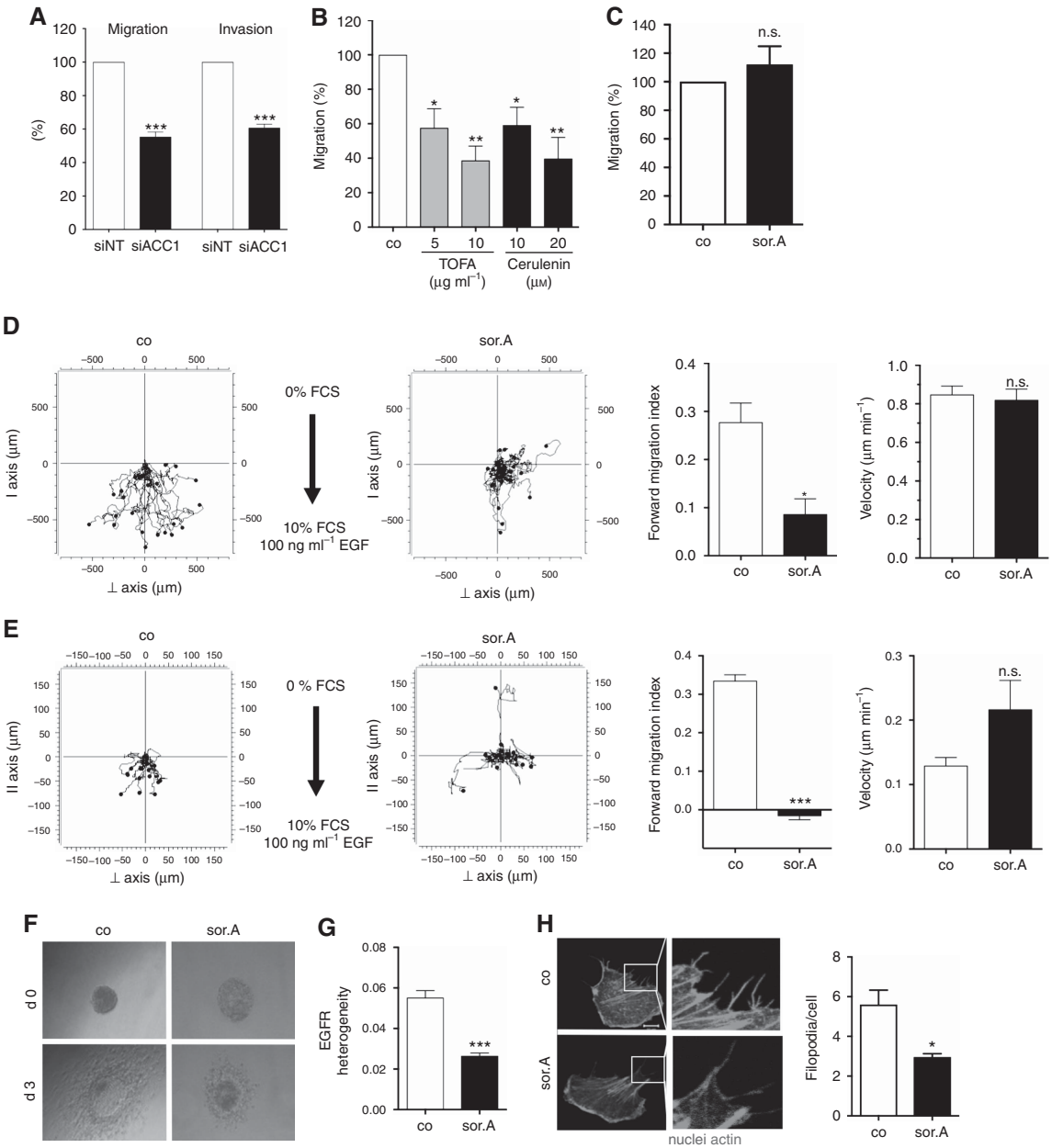

Figure 3. Inhibition of cancer cell migration and invasion by pharmacological targeting of fatty acid synthesis pathway. (**A**) MDA-MB-231 cells were transfected with siRNA against ACC1 and scrambled control, respectively. Migratory and invasive potential of the cells was analysed in transwell assays. (**B**) Treatment with increasing concentrations of the ACC1 inhibitor TOFA and FASN blocker Cerulenin for 72 h strongly diminishes the migration capacity of MDA-MB-231 cells, (**C**) whereas impeding ACC1 activity by 1 μM soraphen A has no effect on the mammary epithelial cell line MCF10a. (**D**) Chemotactic migration and (**E**) invasion of soraphen A-treated MDA-MB-231 cells (1 μM) towards FCS and EGF was investigated by using 2D and 3D chemotaxis slides. Forward migration index and velocity of the cells is shown on the right. (**F**) T24 bladder carcinoma spheroids were embedded in collagen and invasion of the cells towards FCS as chemoattractant was monitored over 3 days. (**G**) Migrating MDA-MB-231 cells treated with or without 1 μM soraphen A were stained with EGFR antibody and localisation of the receptor within the cells was investigated. Heterogeneity was analysed using ImageJ. (**H**) MDA-MB-231 cells were treated with 1 μM soraphen A for 2 h, detached and reseeded. After 2 h cells were fixed and stained with rhodamine phalloidin. Quantification of the number of filopodia is depicted on the right. Error bars show the s.e.m. of three different experiments. Statistical analysis was performed using Student's *t* test: n.s. = non-significant, $*P<0.05$, $**P<0.01$, $***P<0.001$.

Abrogating ACC1 and FASN diminishes proliferation. As pointed out before, cancer cell proliferation is regulated by growth factor receptor signalling cascades and hence might be impaired upon interfering with membrane characteristics. Cellular growth of the breast cancer cell line SKBR3 and the hepatocellular carcinoma cell line Huh7 is significantly inhibited upon treatment with the ACC inhibitor (Figure 4A and B). In accordance, targeting of ACC1 by siRNA (Figure 4C) and the chemical compounds TOFA and CP-640,186, as well as impeding the activity of fatty acid synthase (FASN) by Cerulenin, C75 and UCM05 in SKBR3 cells result in strong impairment of cellular proliferation (Figure 4D). Furthermore, the three-dimensional growth of Huh7 spheroids which were cultivated in poly-HEMA-coated plates is impeded upon treatment with soraphen A (Figure 4E).

To confirm that the changed phospholipid composition is responsible for the growth inhibiting effects of ACC repression, SKBR3 cells were incubated with a mixture of phosphatidylinositol (PI) species, which were demonstrated to be strongly

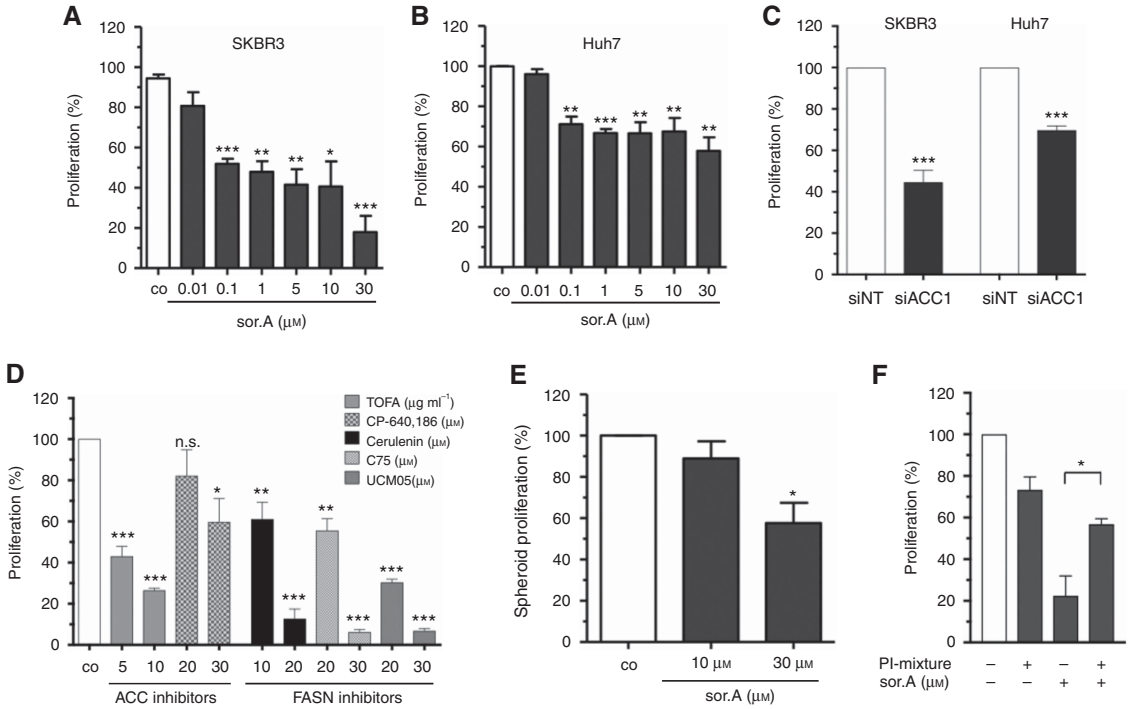

Figure 4. Abrogated proliferative potential. (**A**) SKBR3 and (**B**) Huh7 were treated with increasing concentrations of soraphen A for 96 h and the growth rate was assessed by CellTiter-Blue cell viability assay. (**C**) Cells were transfected with siACC1 or non-targeting siRNA (siNT), respectively. Proliferation of SKBR3 and HuH7 cells was determined after 96 h. (**D**) Proliferation of SKBR3 cells treated with different compounds targeting either ACC1 or FASN was determined. (**E**) Growth of Huh7 spheroids seeded in poly-HEMA plates after stimulation for 96 h. (**F**) Cells were treated with 10 μM soraphen A for 24 h, then 50 μM of a phosphatidylinositol-mixture was added for further 16 h. Medium was changed and proliferation of the cells was investigated after additional 48 h using CellTiter-Blue reagent. Statistical analysis was performed using Student's *t* test: n.s. = non-significant, $*P<0.05$, $**P<0.01$, $***P<0.001$.

downregulated by soraphen A (Figure 1A), in combination with the myxobacterial compound. Whereas the ACC1 inhibitor alone strongly inhibits the growth rate of the cells, combined treatment with PIs significantly reverses the antiproliferative effect of soraphen A (Figure 4F).

***In vivo* efficacy of soraphen A.** In order to transfer the promising *in vitro* data into *in vivo* systems, tumour dissemination as well as xenograft mice experiments were conducted. Thereby, luciferase-tagged 4T1 murine breast cancer cells were pretreated with soraphen A and injected into the tail vein of Balb/c mice. As shown in Figure 5A, whereas control cells disseminate to the lungs, inhibiting fatty acid synthesis by soraphen A abrogated the formation of lung metastasis.

In the last set of experiments, the influence of ACC1 inhibition on tumour growth was analysed. An *in vivo* study utilising SCID mice, which were challenged with Huh7 cells by subcutaneous injection into the flank, revealed that i.p. application of soraphen A is well tolerated by the mice as assessed by body weight (Figure 5B, left-hand side) and importantly, significantly inhibits tumour growth over time (Figure 5B, right-hand side).

DISCUSSION

This study identifies and characterises cellular membranes as an attractive pharmacologically accessible target in anti-cancer therapy. By using chemical inhibitors as well as RNA interference techniques to abrogate the fatty acid synthesis pathway and hence modulating phospholipid composition of cellular membranes, we unravelled the consequences of aberrant membrane physiology on tumour growth and metastasis in detail.

During the last years numerous studies were published regarding cell membrane characteristics within the context of cancer (reviewed in Zalba and Ten Hagen (2017)). Although the so-called membrane lipid therapy, which is described as a new approach to therapeutically target cell membrane composition and structure, is an emerging field in molecular medicine, addressing membrane properties as a well-founded strategy in anti-cancer treatment has not reached the clinic yet (Escriba, 2017). Accordingly, enzymes involved in lipid metabolism might serve as novel promising antineoplastic targets. It was shown that the fatty acid synthase inhibitor Orlistat is able to inhibit growth of breast cancer cells in combination therapies (Menendez *et al*, 2006; Wright *et al*, 2017). A recent publication by the group of Reuben Shaw demonstrated that targeting acetyl-CoA carboxylase (ACC) by applying an allosteric small molecule inhibitor suppressed tumour growth of various non-small-cell lung cancer models *in vivo* (Svensson *et al*, 2016).

Since it is highly intriguing to better understand the functional implications of modified lipid composition and membrane properties with regard to cancer progression, we analysed the crucial importance of phospholipid homeostasis on main tasks of the cell membrane, with special regard to its role in regulating growth factor-mediated signal transduction processes by using the well-known ACC inhibitor soraphen A as a chemical tool. Besides its recently described immunomodulatory and anti-infective effects (Martinez *et al*, 2013; Berod *et al*, 2014; Koutsoudakis *et al*, 2015), soraphen A attracted attention as a potential anti-cancer agent (Beckers *et al*, 2007; Corominas-Faja *et al*, 2014; Daniels *et al*, 2014); however, the underlying molecular mechanism has not been elucidated in detail. The group of Johannes Swinnen actually starts to unravel its mode of action, indicating that targeting ACC changes the phospholipid composition of cellular membranes and interferes with membrane dynamics (Rysman *et al*, 2010). These data could be confirmed by our own study, demonstrating that

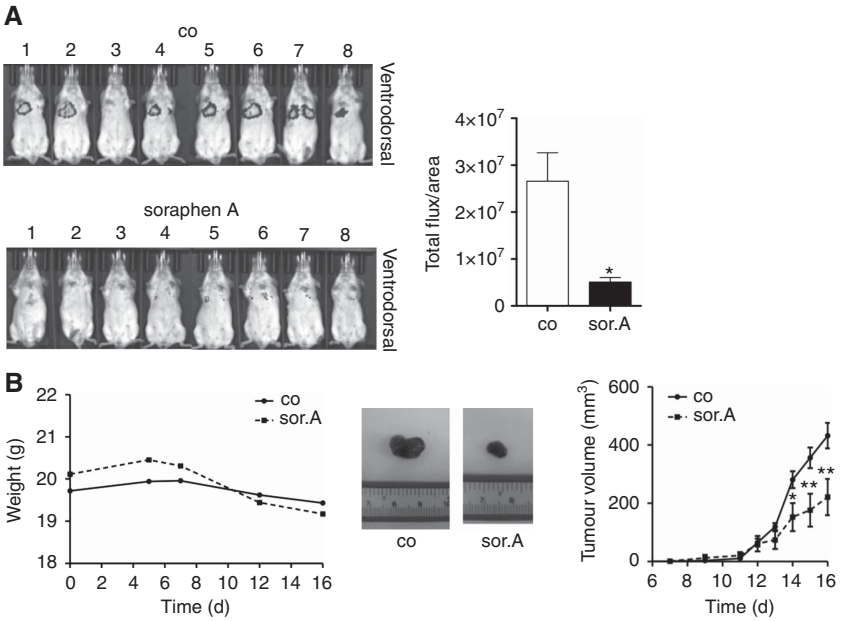

Figure 5. *In vivo* efficacy of soraphen A. (**A**) Soraphen A-treated 4T1-luc cells were injected i.v. into the tail vein of Balb/c mice. Dissemination of the cells to the lungs was monitored after 4 days using the IVIS instrument (Caliper). (**B**) Tumour growth was assessed by using the Huh7 xenograft model. Huh7 cells were injected into the flank of 8-week old SCID mice. After tumours had developed, mice were daily treated i.p. with 40 mg kg^{-1} soraphen A for 9 days. Left: Total weight of soraphen and control-treated SCID mice over time. Right: Tumour growth was measured by evaluating tumour volume over time. Middle: Exemplary pictures of soraphen A- and vehicle-treated tumours at the end of treatment. Statistical analysis was performed using Student's *t* test: *$P<0.05$, **$P<0.01$.

soraphen A modulates the phospholipid composition of cancer cells. Furthermore, cell membrane characteristics such as deformability and lateral fluidity are impaired upon pharmacological targeting or siRNA-mediated inhibition of ACC. Importantly, we extended the data and addressed the consequences of disturbed membrane properties on main tasks of cellular membranes.

Next to simply being a barrier between the cell and its environment, the cell membrane regulates recycling processes and receptor signalling and is the major coordinator between extracellular signals and intracellular responses (Ray *et al*, 2016). Interestingly, we observed that by inhibiting fatty acid biosynthesis, soraphen A not only impedes recycling processes, but also blocks dimerisation and localisation of growth factor receptors. Since dimerisation of growth factors such as HER2 and EGFR is a prerequisite for autophosphorylation of the cytoplasmic domains and subsequent activation of pro-tumourigenic signalling cascades, impeding lateral fluidity of cellular membranes by modulating the phospholipid composition abrogates lateral movement of the receptors, which finally results in impaired downstream signalling and inhibition of cancer progression. Since the efficacy of classical compounds targeting growth factor receptors, such as tyrosine kinase inhibitors (e.g., erlotinib) or monoclonal antibodies against the extracellular domains (e.g., trastuzumab), is often limited due to mutations in the kinase domain of the receptors (Kobayashi *et al*, 2005) or according to signal amplification and diversification (Morgillo *et al*, 2016), interfering with membrane composition in order to prevent receptor dimerisation is a promising novel approach in abrogating growth factor signalling cascades and hence, tumour growth. Moreover, this growth-inhibitory effect of soraphen is amplified by its negative influence on recycling processes. Activated cell surface receptors are internalised, sorted at the endosome and either degraded or recycled back to the membrane in order to promote proliferation. Dysregulated intracellular EGFR trafficking results in mislocalisation of the receptors and aberrant signalling involved in cellular growth and cancer progression (Tomas *et al*, 2014). As shown by transferrin recycling, impairment of ACC activity results in accumulation of the ligand-receptor complexes in the perinuclear compartment, thus further interfering with cancer-associated growth factor receptor signalling.

Extending the study of Scott and colleagues, who showed that impeding ACC activity by using the small molecule TOFA reduces the formation of invadopodia and prevents invasion (Scott *et al*, 2012), we were able to identify the underlying molecular mechanism of impaired migration and invasion upon interfering with fatty acid synthesis and membrane physiology. The formation of filopodia, thin finger-like cytoskeletal protrusions that are filled with actin filaments and known to be essential for migratory processes (Mattila and Lappalainen, 2008), is clearly inhibited by soraphen A. Since mechanical deformation of plasma membrane is required for formation of membrane protrusions (Berro *et al*, 2007), the reduction of membrane deformability by soraphen A certainly has major implications on proper generation of filopodia. Moreover, the localisation of the EGF receptor in migrating cells is significantly changed upon altering membrane properties. During directed migration towards EGF as chemoattractant, its respective receptor (EGFR) is heterogeneously distributed within the cell and known to be mainly localised at the leading edge (Bailly *et al*, 2000). However, treatment with soraphen A decreases the lateral fluidity of cellular membranes and abrogates the proper localisation of EGFR to the leading edge, which finally inhibits EGFR signalling cascades and reduces directed migration and invasion.

To the best of our knowledge, this is the first study describing the *in vivo* efficacy of soraphen A in different mouse models. Dissemination of 4T1 breast tumour cells, which were injected into the tail vain of Balb/c mice, is dramatically impaired after treatment with soraphen A. Although the *in vivo* testing of soraphen A was previously discussed as being hard to address due to its low bioavailability and poor water solubility (Beckers *et al*, 2007), administrating the compound intraperitoneally together with solutol, a non-ionic detergent, and PBS not only is well tolerated by the mice, but even more important, displays potent growth inhibitory effects in a Huh7 liver cancer xenograft mouse model.

In summary, we demonstrated that by altering membrane characteristics through interfering with the fatty acid synthesis

pathway, membrane properties like deformation and fluidity are modulated, which lead to diminished receptor dimerisation, localisation and recycling processes and finally impaired tumour growth and metastasis. Hence, pharmacological targeting of FASN or ACC1 using chemically accessible compounds like soraphen A not only enabled us to obtain deeper knowledge in the role of altered membrane properties in regulating proliferation and metastasis of cancer cells, but based on the impressive *in vivo* efficiency of the ACC1 inhibitor, soraphen A could be introduced as a promising lead substance for anti-cancer agents interfering with membrane physiology.

ACKNOWLEDGEMENTS

We thank Kerstin Loske and Sylvia Schnegg for technical assistance. The experimental contribution of Eva-Maria Baur is gratefully acknowledged. The work was supported by the Deutsche Krebshilfe (SB), Nanosystems Initiative Munich (NIM), and the Deutsche Forschungsgemeinschaft SFB1032, projects A08 (TL) and B08 (SZ).

CONFLICT OF INTEREST

The authors declare no conflict of interest.

REFERENCES

Bailly M, Wyckoff J, Bouzahzah B, Hammerman R, Sylvestre V, Cammer M, Pestell R, Segall JE (2000) Epidermal growth factor receptor distribution during chemotactic responses. *Mol Biol Cell* **11**: 3873–3883.

Beckers A, Organe S, Timmermans L, Scheys K, Peeters A, Brusselmans K, Verhoeven G, Swinnen JV (2007) Chemical inhibition of acetyl-CoA carboxylase induces growth arrest and cytotoxicity selectively in cancer cells. *Cancer Res* **67**: 8180–8187.

Berod L, Friedrich C, Nandan A, Freitag J, Hagemann S, Harmrolfs K, Sandouk A, Hesse C, Castro CN, Bahre H, Tschirner SK, Gorinski N, Gohmert M, Mayer CT, Huehn J, Ponimaskin E, Abraham WR, Muller R, Lochner M, Sparwasser T (2014) De novo fatty acid synthesis controls the fate between regulatory T and T helper 17 cells. *Nat Med* **20**: 1327–1333.

Berro J, Michelot A, Blanchoin L, Kovar DR, Martiel JL (2007) Attachment conditions control actin filament buckling and the production of forces. *Biophys J* **92**: 2546–2558.

Braig S, Schmidt BUS, Katharina S, Chris H, Till M, Oliver W, Rolf M, Stefan Z, Andreas K, Josef AK, Angelika MV (2015) Pharmacological targeting of membrane rigidity: implications on cancer cell migration and invasion. *N J Phys* **17**: 083007.

Cooper GM (2000) *The Cell: A Molecular Approach*. 2nd edn. Sinauer Associates: Sunderland, MA, USA.

Corominas-Faja B, Cuyas E, Gumuzio J, Bosch-Barrera J, Leis O, Martin AG, Menendez JA (2014) Chemical inhibition of acetyl-CoA carboxylase suppresses self-renewal growth of cancer stem cells. *Oncotarget* **5**: 8306–8316.

Daniels VW, Smans K, Royaux I, Chypre M, Swinnen JV, Zaidi N (2014) Cancer cells differentially activate and thrive on de novo lipid synthesis pathways in a low-lipid environment. *PLoS One* **9**: e106913.

Escriba PV (2017) Membrane-lipid therapy: a historical perspective of membrane-targeted therapies – from lipid bilayer structure to the pathophysiological regulation of cells. *Biochim Biophys Acta* **1859**: 1493–1506.

Escriba PV, Busquets X, Inokuchi J, Balogh G, Torok Z, Horvath I, Harwood JL, Vigh L (2015) Membrane lipid therapy: Modulation of the cell membrane composition and structure as a molecular base for drug discovery and new disease treatment. *Prog Lipid Res* **59**: 38–53.

Kobayashi S, Boggon TJ, Dayaram T, Janne PA, Kocher O, Meyerson M, Johnson BE, Eck MJ, Tenen DG, Halmos B (2005) EGFR mutation and resistance of non-small-cell lung cancer to gefitinib. *N Engl J Med* **352**: 786–792.

Koeberle A, Shindou H, Koeberle SC, Laufer SA, Shimizu T, Werz O (2013) Arachidonoyl-phosphatidylcholine oscillates during the cell cycle and counteracts proliferation by suppressing Akt membrane binding. *Proc Natl Acad Sci USA* **110**: 2546–2551.

Koutsoudakis G, Romero-Brey I, Berger C, Perez-Vilaro G, Monteiro Perin P, Vondran FW, Kalesse M, Harmrolfs K, Muller R, Martinez JP, Pietschmann T, Bartenschlager R, Bronstrup M, Meyerhans A, Diez J (2015) Soraphen A: a broad-spectrum antiviral natural product with potent anti-hepatitis C virus activity. *J Hepatol* **63**: 813–821.

Martinez JP, Hinkelmann B, Fleta-Soriano E, Steinmetz H, Jansen R, Diez J, Frank R, Sasse F, Meyerhans A (2013) Identification of myxobacteria-derived HIV inhibitors by a high-throughput two-step infectivity assay. *Microb Cell Fact* **12**: 85.

Mattila PK, Lappalainen P (2008) Filopodia: molecular architecture and cellular functions. *Nat Rev Mol Cell Biol* **9**: 446–454.

Menendez JA, Vellon L, Lupu R (2006) The antiobesity drug Orlistat induces cytotoxic effects, suppresses Her-2/neu (erbB-2) oncogene overexpression, and synergistically interacts with trastuzumab (Herceptin) in chemoresistant ovarian cancer cells. *Int J Gynecol Cancer* **16**: 219–221.

Morgillo F, Della Corte CM, Fasano M, Ciardiello F (2016) Mechanisms of resistance to EGFR-targeted drugs: lung cancer. *ESMO Open* **1**: e000060.

Pernpeintner C, Frank JA, Urban P, Roeske CR, Pritzl SD, Trauner D, Lohmuller T (2017) Light-controlled membrane mechanics and shape transitions of photoswitchable lipid vesicles. *Langmuir* **33**: 4083–4089.

Ray S, Kassan A, Busija AR, Rangamani P, Patel HH (2016) The plasma membrane as a capacitor for energy and metabolism. *Am J Physiol Cell Physiol* **310**: C181–C192.

Remmerbach TW, Wottawah F, Dietrich J, Lincoln B, Wittekind C, Guck J (2009) Oral cancer diagnosis by mechanical phenotyping. *Cancer Res* **69**: 1728–1732.

Rysman E, Brusselmans K, Scheys K, Timmermans L, Derua R, Munck S, Van Veldhoven PP, Waltregny D, Daniels VW, Machiels J, Vanderhoydonc F, Smans K, Waelkens E, Verhoeven G, Swinnen JV (2010) De novo lipogenesis protects cancer cells from free radicals and chemotherapeutics by promoting membrane lipid saturation. *Cancer Res* **70**: 8117–8126.

Scott KE, Wheeler FB, Davis AL, Thomas MJ, Ntambi JM, Seals DF, Kridel SJ (2012) Metabolic regulation of invadopodia and invasion by acetyl-CoA carboxylase 1 and de novo lipogenesis. *PLoS One* **7**: e29761.

Steigemann P, Wurzenberger C, Schmitz MH, Held M, Guizetti J, Maar S, Gerlich DW (2009) Aurora B-mediated abscission checkpoint protects against tetraploidization. *Cell* **136**: 473–484.

Suresh S (2007) Biomechanics and biophysics of cancer cells. *Acta Biomater* **3**: 413–438.

Svensson RU, Parker SJ, Eichner LJ, Kolar MJ, Wallace M, Brun SN, Lombardo PS, Van Nostrand JL, Hutchins A, Vera L, Gerken L, Greenwood J, Bhat S, Harriman G, Westlin WF, Harwood Jr. HJ, Saghatelian A, Kapeller R, Metallo CM, Shaw RJ (2016) Inhibition of acetyl-CoA carboxylase suppresses fatty acid synthesis and tumor growth of non-small-cell lung cancer in preclinical models. *Nat Med* **22**: 1108–1119.

Swaminathan V, Mythreye K, O'Brien ET, Berchuck A, Blobe GC, Superfine R (2011) Mechanical stiffness grades metastatic potential in patient tumor cells and in cancer cell lines. *Cancer Res* **71**: 5075–5080.

Tomas A, Futter CE, Eden ER (2014) EGF receptor trafficking: consequences for signaling and cancer. *Trends Cell Biol* **24**: 26–34.

Wright C, Iyer AKV, Kaushik V, Azad N (2017) Anti-tumorigenic potential of a novel orlistat-AICAR combination in prostate cancer cells. *J Cell Biochem* **118**: 3834–3845.

Zalba S, Ten Hagen TL (2017) Cell membrane modulation as adjuvant in cancer therapy. *Cancer Treat Rev* **52**: 48–57.

Supplementary Information accompanies this paper on British Journal of Cancer website (http://www.nature.com/bjc)